

# Time-resolved fluorescence lifetime imaging microscopy using a picosecond pulsed tunable dye laser system

Ammasi Periasamy, Pawel Wodnicki, Xue F. Wang, Seongwook Kwon, Gerald W. Gordon, and Brian Herman<sup>a)</sup>

Laboratories for Cell Biology, Department of Cell Biology and Anatomy, CB# 7090, University of North Carolina, School of Medicine, Chapel Hill, North Carolina 27599

(Received 25 April 1996; accepted for publication 24 June 1996)

The design and implementation of a time-resolved fluorescence lifetime imaging microscope (TRFLIM) for the biomedical sciences are described. The measurement of fluorescence lifetimes offers many benefits, among which is that they are independent of local signal intensity and concentration of the fluorophore and they provide visualization of the molecular environment in a single living cell. Unlike single photon counting, which employs a photomultiplier as the detector, TRFLIM uses a nanosecond-gated multichannel plate image intensifier providing a two-dimensional map of the spatial distribution of fluorescent lifetime in the sample under observation. Picosecond laser pulses from a tunable dye laser are delivered to the fluorophore inside living cells on the stage of a fluorescent microscope. Images of the fluorescence emission at various times during the decay of the fluorescence are collected using a high-speed gated image intensifier and the lifetimes are calculated on a pixel-by-pixel basis. Lifetimes measured by TRFLIM are compared with those measured by conventional methods. © 1996 American Institute of Physics. [S0034-6748(96)03610-6]

## I. INTRODUCTION

Fluorescence microscopy provides a sensitive means of acquiring information about the molecular organization of cells and tissues. Recent advances in fluorescence microscopy now permit quantitative measurement and acquisition of spectroscopic information from the sample under study in two- or three-dimensions. This has resulted in the fluorescence microscope becoming a highly useful tool for the sensitive detection of a number of properties of biological specimens.<sup>1-5</sup> Time-resolved fluorescence lifetime measurements are a valuable part of the repertoire of fluorescence microscopy.

Several fluorescent probes change their lifetimes in response to specific intracellular factors such as  $[H^+]$ ,  $[Ca^{2+}]$ ,  $[O_2]$ , membrane potential, temperature, polarity of the probe environment, and alterations in the conformation and interactions of macromolecules.<sup>6,7</sup> Lifetime measurements of the probes allow the quantitative determination of the intracellular factors.

Current methods for measuring fluorescence lifetimes employ either frequency-domain<sup>8-10</sup> or time-domain<sup>11</sup> methods. In frequency-domain lifetime measurements, the sample is excited with radio frequency (for nanosecond decays) sinusoidally modulated light, and the phase shift and amplitude attenuation of the fluorescence emission relative to the phase and amplitude of the exciting light are measured. Each fluorophore lifetime causes a unique phase shift and attenuation at a given frequency. In time-domain methods, pulsed light is used as the excitation source and fluorescence lifetimes are measured from the fluorescence decay signal di-

rectly or by single photon counting (SPC). These conventional approaches allow measurement of fluorescence lifetimes with high temporal resolution, but are severely limited in their ability to provide spatial information. Time-resolved fluorescence lifetime imaging (TRFLIM) is an extremely important advance as it allows environmental parameters to be monitored in a spatially defined manner in the specimen under study (i.e., a single living cell). Recent technological advances in high-speed pulsed lasers with picosecond and femtosecond pulse width and rapid and variable repetition rates, as well as high speed sensitive image detection devices and highly specific fluorescent probes and image processing techniques, have facilitated the development of TRFLIM. As we describe here, the algorithm for calculation of two-dimensional (2D) lifetime images is simple and easy to implement, compared to the curve fitting methods employed in analysis of phase modulation and single photon counting data. We describe the design and implementation of the TRFLIM for measurements of the fluorescent lifetime in two-dimensions, resulting in the generation of images in which the brightness of color of each pixel is a function of the lifetime measured in that pixel. We also compare the TRFLIM data with SPC measurements of the same sample to determine the accuracy of TRFLIM measurement of fluorescent lifetimes.

## II. PRINCIPLE OF TRFLIM

The fluorescence lifetime ( $\tau$ ) is the characteristic time that a molecule remains in an excited state prior to returning to the ground state. For single exponential decay of fluorescence, after a brief pulse of excitation light, the fluorescence intensity as a function of time is described as

$$I(t) = I_0 \exp(-t/\tau), \quad (1)$$

<sup>a)</sup>Also at: Cell Biology Program, Lineberger Comprehensive Cancer Research Center, University of North Carolina, School of Medicine, Chapel Hill, NC 27599; Electronic mail: bhgf@med.unc.edu

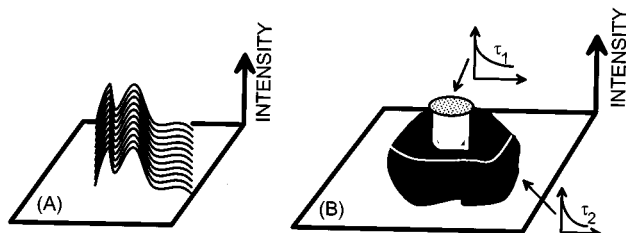


FIG. 1. Basic principle of time-resolved fluorescence lifetime imaging. Two environmentally distinct regions of a microscopic sample labeled by a fluorescent probe are illustrated by (A) a three-dimensional intensity plot, and (B) a lifetime image. In this hypothetical case, intensity measurements demonstrate nonuniform intensity throughout the cell with no correlation with the distinct environmental regions. The environmentally distinct regions of the sample,  $\tau_1$  and  $\tau_2$ , are clearly differentiated in lifetime imaging (B).

where  $I_0$  is the initial intensity immediately after the excitation pulse. The fluorescence lifetime ( $\tau$ ) is defined as the time in which the fluorescence intensity decays to  $1/e$  of the initial intensity ( $I_0$ ).

Both frequency-domain and time-resolved methods have been used to measure fluorescent lifetimes in a variety of different samples. However, when examining biological samples (cells or tissues), it is highly advantageous to be able to monitor the spatial heterogeneity in the fluorescent lifetime. Consider the case where a fluorophore in a microscopic sample (i.e., a cell) exists in two environmentally distinct regions, but has a fluorescence intensity distribution which is not correlated with the distribution of fluorescent lifetime [Fig. 1(A)]. However, the fluorescence lifetime ( $\tau_1$ ) in the central region of the sample is longer than that in our outer region [ $\tau_2$ , Fig. 1(B)]. Since the fluorophore has a similar intensity distribution in the two regions, measurements of fluorescence intensity would not reveal any difference between the two regions. However, imaging of the fluorescence lifetime would allow discrimination of the two different regions [Fig. 1(B)]. A nonuniform distribution of the probe resulting in spatial variations in intensity may lead to incorrect intensity based measurements of the probe's environment. Fluorescence lifetime measurements can give correct values under these circumstances.

### III. BASIC ELEMENTS OF TRFLIM

A schematic of the TRFLIM instrumentation is shown in Fig. 2. In this section we describe the hardware and software comprising the system—a picosecond laser, microscope, high-speed gated image intensifier, and other components required for TRFLIM or SPC.

#### A. Laser system

A brief introduction of the laser system is necessary to understand the synchronization of the laser system with other instrumentation such as the high speed gated image intensifier (see Sec. II C) and SPC data collection. The laser system consists of an yttrium aluminum garnet (YAG) laser, second harmonic generator (SHG), mode locker, dye laser, cavity dumper, and other electronics (see Fig. 2). The folded resonator design cw Nd:YAG laser (Antares 76-S, Coherent Inc.,

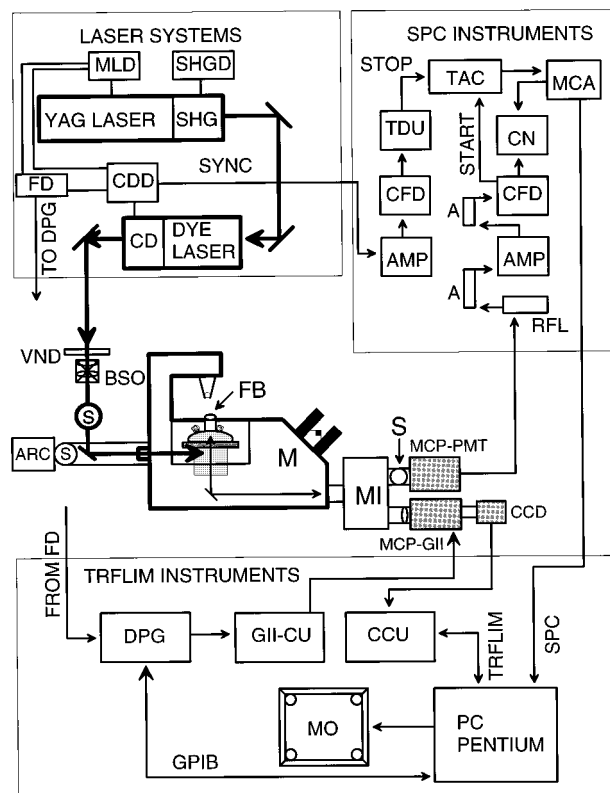


FIG. 2. Schematic diagram of time-resolved fluorescence lifetime imaging microscope (TRFLIM). A tunable picosecond (ps) pulsed dye laser system (see the text for details) provides 6 ps excitation pulses at repetition rates of up to 76 MHz. The laser light is coupled to the Nikon inverted microscope (M) through the variable neutral density filter (VND), beam steering optics (BSO), and the shutter (S) controlled via software. Lifetime measurements were obtained by SPC or TRFLIM. In TRFLIM the reference signal (9.277 kHz repetition rate) from the frequency divider (FD) is used to trigger a delay pulse generator (DPG), which provides a delayed TTL pulse to the gated image intensifier control unit (GII-CU) to control the gate duration of the single stage microchannel plate gated image intensifier (MCP-GII). The DPG settings (delay time and pulse width) are computer (PC PENTIUM) controlled through a general purpose interface bus (GPIB) to allow automated collection of time-resolved images. The lifetime image is generated from the time-resolved images collected by a high-speed gated image intensifier (MCP-GII) lens coupled to a cooled charge-coupled device digital camera (CCD). For SPC the STOP signal is generated from the cavity dumper driver unit (CCD) SYNC signal. The START signal is generated from the fluorescence signal detected by the two-stage microchannel plate photomultiplier tube (MCP-PMT). MLD is the mode locker driver; SHG the second harmonic generator and the driver (SHGD); THG the third harmonic generator; CD the cavity dumper; ARC the arc lamp; FB the fluorescent probe or specimen; MI the multi image module; RFL the RF limiter; A the attenuator; AMP the amplifier; CFD the constant fraction discriminator; TDU the time delay unit; CN the counting unit; TAC the time to amplitude converter; MCA the multichannel analyzer; MO the monitor; and CCU the camera control unit.

CA) is mode-locked using a Coherent mode locker (model 7600) at 38 MHz producing output pulses at 76 MHz. The mode-locked IR power is 24 W, TEM<sub>0,0</sub> mode with less than 1% peak-to-peak noise. The laser pulses are monitored with a fast photodiode (AR-S3; Antel, Canada) whose output is monitored with a Tektronix CSA 803 digital sampling oscilloscope (CSA 803A Communications Signal Analyzer with an SD-26 sampling head). The response time of this detection system is 45 ps full width at half maximum and properly mode-locked laser pulses yield smooth traces of 80–100 ps

TABLE I. Excitation, dichroic, and emission filters used for TRFLIM.

Probe	Excitation wavelength (nm)	Dichroic ( $\lambda$ ) filter (nm)	Emission filter (LP) <sup>a</sup> (nm)
Calcium Crimson	585	610	610
Calcium Green	490	510	520
Calcium Orange	560	580	590
Rhodamine B and Rose Bengal	570	580	590

<sup>a</sup>LP denotes long pass.

FWHM. A Coherent temperature controlled second harmonic generator (SHG, model 7900) provides a stable high power source of second harmonic (green, 532 nm) mode-locked laser light pulses. The polarization rotation and discrimination assembly used in the 532 nm output rotates the polarization of the second harmonic beam (3 W, 80 ps FWHM) into the vertical direction, suitable for dye laser pumping. To pump the R6G dye, we employed the configuration shown in Fig. 2 in which the IR and green laser lines are separated by using a half-wave plate and IR/green beam splitter.

Optimal conditions for generating short pulses are achieved by accurately matching cavity lengths of the dye and the pumping lasers. Precision adjustment of the cavity length of dye laser is most easily performed while monitoring the laser pulses with a real time autocorrelator. The dye laser can operate at a wide range of wavelengths depending on the dye employed. The desired wavelength is tuned in the 700 dye laser using a single or double plate birefringent filter in the cavity. R6G dye pumped by the 2 W SHG line (532 nm,  $\sim$ 80 ps pulse width) emits  $\sim$ 300 mW at 590 nm (with tunable range 560–610 nm) with a pulse width (measured with a Femtochrome model FR103 autocorrelator) of  $\sim$ 6 ps at 3.8 MHz cavity dumper repetition rate.

The excitation laser pulse width increases with decreasing repetition rate; for example, at 10 kHz cavity dumper repetition rate the width increases by 20–30%. The laser pulse width also increases when the laser beam is coupled to the microscope through beam steering optics or fiber optics.

## B. Microscope

The microscope (Nikon Diaphot 300) has two illumination ports, one for an arc lamp for conventional fluorescence imaging and the other for the laser for time-resolved lifetime microscopy. The microscope optics have the ability to transmit from near UV to near IR. The laser light is coupled to the microscope by beam steering optics (BSO). The different filter combinations (Omega Optics, Brattleboro, VT) used in the TRFLIM are listed in Table I. The output port of the microscope is connected directly to either a microchannel plate photomultiplier tube (MCP-PMT) (for SPC) or a microchannel plate high-speed gated image intensifier (for TRFLIM). It is possible to use a multi-image module (MI) with a 50% beam splitter for simultaneous data collection, but light loss and internal reflections within the multi-image module significantly decrease the sensitivity and accuracy of the lifetime measurement. A 40X oil, 1.3 numerical aperture (NA) objective lens is used for experiments; oil and non-

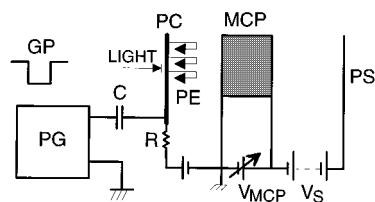


FIG. 3. Schematic of shutter operation of gated image intensifier (see the text for details). GP is the gate pulse; PG the pulse generator; PE the photoelectrons; PC the photocathode; MCP the microchannel plate; and PS the phosphor screen.

phase objectives should be used to minimize any light scattering in the objective lens. The microscope, multi-image module, and detectors are mounted on a Newport vibration isolation table. Both the input and output of the microscope are equipped with shutters which are used to limit exposure of the sample and detectors to potentially damaging illumination. The walls of the room are painted flat black to reduce the stray light or laser light scattered from beam steering mirror surfaces from reaching the detector or the users.

## C. High-speed gated image intensifier and video camera

The microchannel plate gated image intensifier (MCP-GII) has two modes of operation, continuous (nongated) for conventional fluorescence intensity imaging and gated for TRFLIM operation. Gating action (see Fig. 3) is achieved by controlling the potential of the photocathode (PC) with respect to the input surface of the MCP. In an OFF state positive photocathode potential prevents photoelectrons (PE) from entering the MCP while in an ON state this potential is reversed and electrons enter the MCP, where they undergo multiplication and then strike the phosphore screen (PS) forming an optical image. The low resistivity photocathode employed in the MCP-GII minimizes the iris effect (shading error) during this high speed gating.<sup>12</sup> Generation of the gating voltage ( $V_G$ ) is controlled by a TTL pulse (positive logic, 5 V peak to peak maximum), and the gate width can be varied from 3 ns to 100  $\mu$ s (2 ns rise time, 3 ns fall time, and  $\leq$ 200 ps jitter) with a maximum repetition rate of 10 kHz (due to the phosphorscreen persistence). The MCP-GII photocathode lumen sensitivity is 150  $\mu$ A/lm, the minimum image intensification is 5000 (MCP voltage of 900 V), and it is spectrally responsive from 180 to 840 nm (quantum efficiency at 620 nm is 9%).

The MCP-GII is lens coupled to a dual-mode cooled, frame transfer charge-coupled device (CCD) camera (C4880, Hamamatsu). The camera is thermoelectronic and water cooled to  $-30$   $^{\circ}$ C to suppress the noise due to dark current and enable a much higher signal to noise (S/N) ratio and a wider dynamic range (1:5000) than an ordinary line transfer CCD camera. It has two readout modes a high precision low-speed mode (maximum 4 s/frame) with 12–14 bits of resolution and a high-speed mode (up to 7 frames/s) with 10 bit resolution. The CCD chip has a sensitive area of 12 mm  $\times$  12.2 mm, which is comprised of square (12  $\mu$ m  $\times$  12  $\mu$ m) pixels arranged in matrix of 1000 lines and 1018 columns. For TRFLIM, it is essential to have a resolution  $\geq$ 10 bits.

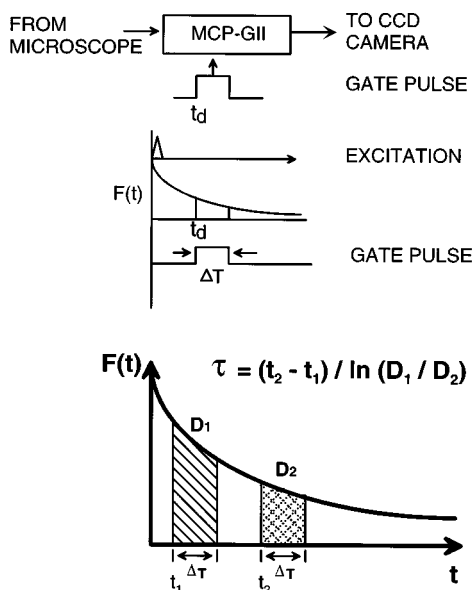


FIG. 4. Functional description of TRFLIM image detection using a gated MCP image intensifier (see the text for details).

The camera provides a 16 bit digital output (RS-422A), allowing images to be input directly into a digital input frame grabber board (Matrox Image 1280 baseboard with ASD). In the high precision mode this camera is capable of low (25 electrons/AD count), high (5 electrons/AD count), and super-high gain (1 electron/AD count), operation which is useful for adjusting the instrument and focusing the microscope. The camera has a broad spectral response from 200 to 1100 nm with 27% quantum efficiency at 620 nm.

#### D. Theory of rapid lifetime determination and image acquisition

A monoexponential decay of the fluorescence signal excited by a short pulse of excitation can be written as

$$F(t) = A \exp(-t/\tau). \quad (2)$$

In the imaging mode, however, using nonlinear curve fitting methods, extracting parameters  $A$  and  $\tau$  from the enormous number of data points is time consuming. A basic description of how rapid lifetime determination using multigate detection is accomplished is shown in Fig. 4. The fluorescence decay is detected at two different delay times  $t_1$  and  $t_2$  with the gate width  $\Delta T$ . The gated fluorescence signals ( $D_1$  and  $D_2$ ) can be described as

$$D_1 = \int_{t_1}^{t_1 + \Delta T} A \exp(-t/\tau) dt, \quad (3)$$

$$D_2 = \int_{t_2}^{t_2 + \Delta T} A \exp(-t/\tau) dt. \quad (4)$$

The lifetime  $\tau$  and preexponential factor  $A$  can be extracted as follows:

$$\tau = (t_2 - t_1) / \ln(D_1/D_2), \quad (5)$$

$$A = (D_1/\tau) \exp(-t_1/\tau) [1 - \exp(\Delta T/\tau)]. \quad (6)$$

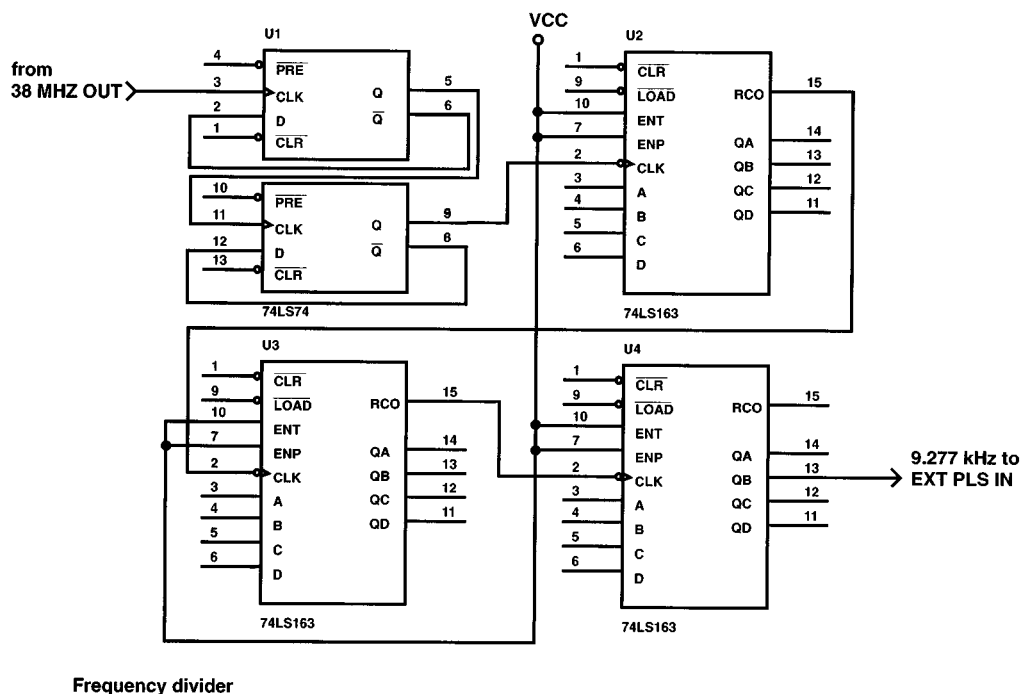
Using this method results in extremely short calculation times. The average fluorescence lifetimes and preexponential factors can be calculated directly from only four parameters ( $D_1$ ,  $D_2$ ,  $t_1$ , and  $t_2$ ) without doing iterative deconvolution as required by conventional nonlinear least squares analysis.<sup>13-19</sup>

The fluorescently labeled specimen (or solution of fluorescent probe) in a specially designed chamber<sup>1</sup> is placed on the microscope stage. The average power of the laser at the specimen plane ( $500 \mu\text{W}$  at 10 kHz) should be carefully selected to reduce any photodamage or photobleaching of the specimen. The synchronization of the MCP-GII gating to the excitation of the specimen by the laser pulse as well as gate duration selection is achieved using a digital delay pulse generator (DDPG-353, Stanford Research systems, CA) (see Figs. 2 and 4). Following delivery of an excitation pulse, the MCP-GII is turned on for a very brief interval ( $\Delta T$ ) at some delay time ( $t_1$ ) after the exciting pulse and the emitted intensity from the MCP-GII is acquired on the cooled CCD (which is continually left on) (Fig. 4). This process is repeated a large number of times (e.g., 10 000 laser pulses), allowing accumulation of the image on the CCD chip to a level of S/N ratio that permits digitization with desired bit resolution, and then the digitized image is read out and stored as an image of the first gate. The image derived from the second gate is collected in the same way after changing the delay time ( $t_2$ ,  $t_2 > t_1$ ) when the MCP-GII is turned on. To obtain a lifetime image, the two time shifted gate images are processed on a pixel by pixel basis as described in Sec. V, and the image is displayed on the color monitor.

#### E. Single photon counting

The measurement of fluorescence lifetime by SPC is an established technique.<sup>7,20</sup> An SPC instrument has been developed to verify data collected by TRFLIM. A brief introduction to the hardware and software will indicate the requirements for measuring lifetimes using SPC through the microscope and in living cells.

A block diagram of the SPC instrumentation is shown in Fig. 2. In the reverse mode configuration,<sup>2,11,21</sup> the start signal is generated by the first single photon (fluorescence from the excited fluorophores in the specimen), detected by an MCP PMT (R3809U, Hamamatsu Photonics, NJ), which is amplified (model HP 8447F; 1.3 GHz) and sent to a time-to-amplitude converted (TAC) (model TC 864, Oxford-Tennelec Instruments, TN). The stop signal is generated from the excitation pulse detected by a  $p-i-n$  photodiode (model DET2-SI; Thorlabs, Newton, NJ) or a SYNC pulse from the DC driver, which is delayed for a defined period that is greater than the time required for detection of the first emitted single photon. The TAC in turn provides a voltage pulse whose amplitude is proportional to the time elapsed between the start and stop signals. The amplitude of this pulse is stored in a multichannel analyzer (MCA, model PCA II) installed in a PC computer (Insight). This cycle is repeated a large number of times, yielding a histogram of the individual lifetimes of excited fluorophore molecules accumulated in the MCA. The histogram has an exponential form



Frequency divider

FIG. 5. Circuit diagram of external frequency divider. Frequency divider allows the operation of the laser at a 9.277 kHz repetition rate and provides a jitter-free trigger signal for delay pulse generator (DPG).

and is directly related to the fluorescence decay curve of the sample.

To achieve single photon detection and avoid pileup, the level of incident fluorescence intensity delivered to the MCP-PMT should be low. A simple rule of thumb is to limit the count rate at the constant fraction discriminator (CFD; model TC 454) to no more than 10% of the exciting laser pulse repetition frequency. The internal CFD delay should be set by the manufacturer of the discriminator for a given PMT. The time calibration of each channel in the MCA is done by using time delay units.<sup>11</sup>

#### IV. SELECTION OF THE LASER REPETITION RATE

The laser pulse repetition rate determines the time required for data collection and in general it should be as high as possible in order to achieve good time resolution. However, experimental conditions may limit the usable repetition rate.

The methods available to vary the laser repetition rate are an electro-optic shutter, pulse picker, or cavity dumper. The Coherent 7220 cavity dumper (CD) unit (as shown in Fig. 2) is used in synchronously pumped dye laser systems to provide selectable output pulse repetition rates. The pulse repetition rate can be selected using the internal triggering of the CD driver from 146.7 kHz and 38 MHz or external triggering, which allows selection of any repetition rate from 1 Hz to 38 MHz.

In case of the SPC measurements, the maximum conversion rate of the time to amplitude converter (TAC; TC 864 Tennelec/Nucleus Inc., Oak Ridge, TN) and the analog to digital (A/D) converter in the MCA card<sup>22</sup> are likely to limit the maximum count rate and thus the repetition rate. If in-

strumentation is fast, incomplete sample recovery between pulses in systems in which long-lived transients are formed<sup>23,24</sup> may limit the laser repetition rate (though there are ways to collect data at a high repetition rate<sup>25</sup>). For the SPC measurements reported here, the range of the internal triggering of the CD driver proved adequate to select the suitable laser repetition rate.

For TRFLIM measurements the limiting factor is the maximum repetition rate of the MCP-GII, which is only 10 kHz. With internal triggering of the CD driver it is possible to achieve a minimum repetition rate of 146.7 kHz, and in order to match the laser repetition rate to the MCP-GII it was necessary to provide an external trigger signal to the CD driver. The external trigger signal can be provided from the digital delay pulse generator (DDPG-353, Stanford Research Systems, CA) as a 10 kHz TTL signal, which is fed into the EXT PLS IN input on the CD driver. However, because of the lack of synchronization with the mode-locker signal of the laser this configuration introduces jitter (26 ns) between the SYNC output from the CD driver unit and the laser pulse. A frequency divider circuit was designed (Fig. 5; also Fig. 2) to obtain required laser repetition rate and a jitter-free SYNC signal to trigger the MCP-GII by externally dividing 38 MHz mode-locker signal.

#### V. SYSTEMS EVALUATION

TRFLIM was used to collect lifetime data of Rhodamine B (RdB) and Rose Bengal (RsB) in different solvents (1  $\mu$ M solution). Figure 6 illustrates a series of fluorescence intensity images obtained at various times during the decay of the excited state of RdB in ethanol at room temperature. Images of the different gate windows were acquired using custom

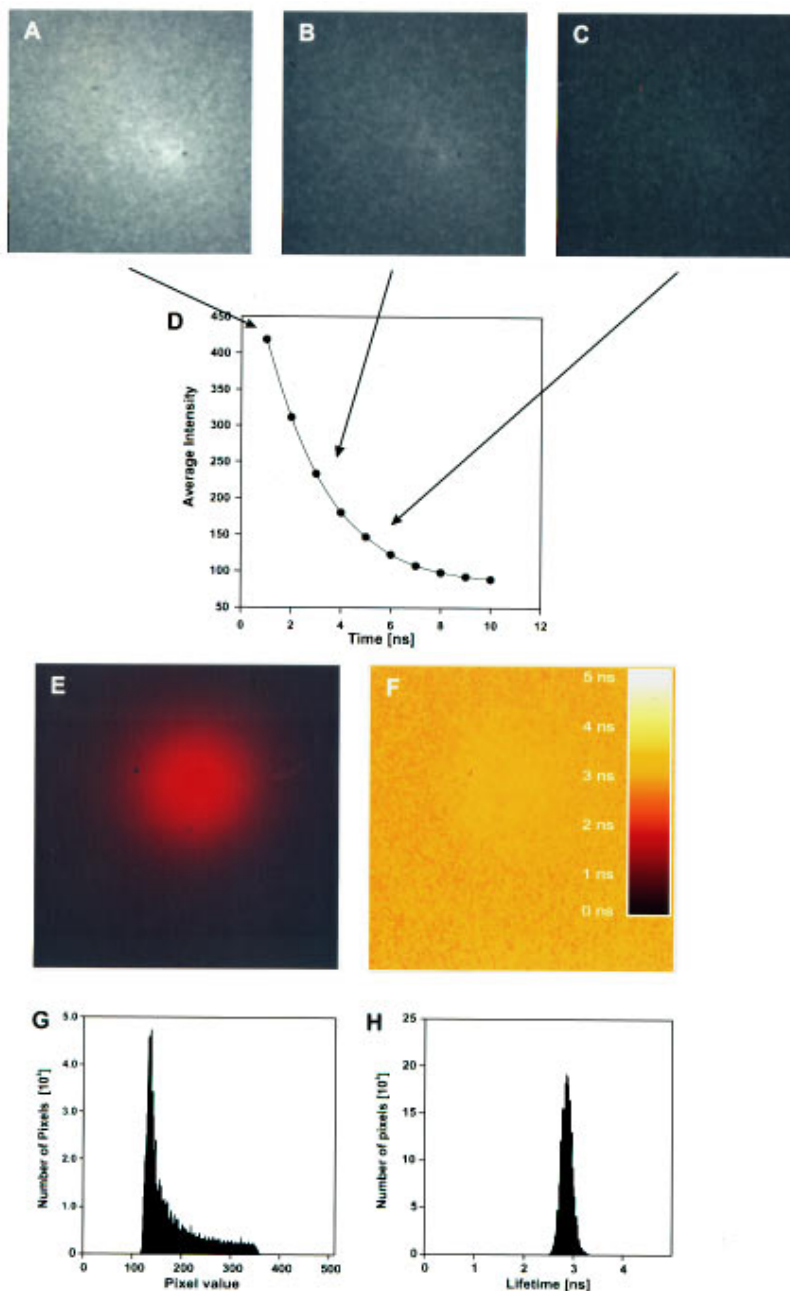


FIG. 6. Fluorescent intensity and lifetime images of Rhodamine B (RdB). A  $1 \mu\text{M}$  solution of RdB was prepared in ethanol and imaged using TRFLIM at room temperature. (A)–(C) Time-resolved fluorescence intensity images of RdB at various times (1, 3, and 6 ns) after the laser excitation pulse. The intensity of the images decreases as the time between the excitation pulse and turning on of the gated image intensifier increases. (D) The decay of fluorescence intensity with time following excitation ( $t=0$ ). Typical intensity (E) of lifetime (F) images and their respective histograms (G) and (H), lifetime images of RdB was derived from two time-resolved images. The RdB lifetime value of 2.88 ns was determined from the position of the peak of the histogram. Note the different shape and character of the histograms of the intensity image and the lifetime image. The intensity histogram has a peak that corresponds to a large number of background pixels while intensities of other pixels are quite uniformly distributed over a range of values. In contrast, the lifetime image histogram consists only of a well defined, symmetrical, and narrow peak with the shape of the Gaussian distribution.

image acquisition software. Using the camera at 12 bit resolution improves the accuracy of data analysis but limits time resolution of a series. Using 10 bit resolution speeds image acquisition considerably without sacrificing too much accuracy; 8 bit resolution proved to be unacceptable for lifetime imaging. Data collection is automated through custom software allowing a series of images to be acquired at different time delays during the fluorescence lifetime. The images and a background image were stored on a hard disk for later processing.

Determination of lifetime values is by the rapid lifetime measurement method.<sup>13</sup> In this method the one component lifetime value is proportional to the ratio of two gate window images. To minimize noise<sup>13</sup> a gate width of 2.5 times the lifetime should be used and gates should be separated by 2.5 times the lifetime. After image collection, a background image is subtracted from all images in the series; this step is necessary to remove the autofluorescence and electronic noise in the image. Thresholding (typically 10% above the background) of the background-subtracted image is then per-

TABLE II. Comparison of literature and measured lifetimes using different measurement techniques.

Probes <sup>a</sup>	SPCM <sup>b</sup> (ns)	FLIM <sup>c</sup> (ns)	FM <sup>d</sup> (ns)	Literature (ns)
Rhodamine in ethanol	2.9	3	2.9	2.88, <sup>e</sup> 3.2, <sup>f</sup> 2.3 <sup>f</sup>
Rose Bengal (RsB) in acetone	2.5	2.4	2.6	2.57 <sup>h</sup>
RsB in <i>N,N</i> , dimethyl formamide	2.2	2.2	2.3	2.19 <sup>h</sup>
RsB in 2-propanol	1.0	1.1	1.1	0.975 <sup>h</sup>
RsB in ethanol	0.8	0.8	0.8	0.739 <sup>h</sup>

<sup>a</sup>At room temperature.

<sup>b</sup>SPCM denotes single photon counting microscopy.

<sup>c</sup>FLIM denotes fluorescence lifetime imaging microscopy.

<sup>d</sup>FM denotes frequency modulation.

<sup>e</sup>Reference 29.

<sup>f</sup>Reference 30.

<sup>g</sup>Reference 31.

<sup>h</sup>Reference 32.

formed (to remove noisy pixels) and then two gate images are chosen for ratioing. The ratios are calculated on a pixel by pixel basis to form the lifetime image. If more than two gate images were collected, lifetimes can be derived from the ratio of any of the gate window images. Ideally lifetime images formed from any pair of the gate window images should be identical; however, in practice, images that are too close to one another in time as well as images that are collected from the tail of the fluorescence decay produce lifetime images of poor quality (low S/N) and should be avoided. The average lifetime of RdB obtained by TRFLIM was 3 ns (Table II). According to the above discussion the optimum gate width of the MCP-GII should be 7.5 ns. To demonstrate relation between the S/N ratio of the lifetime image and gate width, we collected a series of time-resolved images of RdB solution with gate width varying from 3 to 11 ns, separated by  $\Delta T$  equal to the gate width (Fig. 7). The quality of the lifetime images as measured by the histogram width is best for the images formed from gate images of 7 and 8 ns width, which is in excellent agreement with the theoretical prediction.<sup>13</sup>

To optimize the performance of the PMT in SPC, the following procedures should be followed when setting up the instrument. Proper operation of the MCP-PMT is verified by operating the PMT in a dark environment and monitoring the output current on an oscilloscope (model 2467B, 400 MHz, Tektronix) while gradually increasing the supply voltage. It is important to keep the laser light intensity and repetition frequency such that the output current from the MCP-PMT does not exceed 100 nA.

Before beginning an experiment, the instrument is allowed to warm up for a half hour to allow for thermal equilibration of the equipment. In SPC, when deconvolution of the experimental data is required, the instrument response function (IRF) must be representative of the condition of the equipment during the recording of the fluorescence decay. Obtaining an accurate IRF is straightforward for solution samples and can be done by replacing the sample with a scattering solution such as nondairy coffee creamer. The two samples (specimen and the scatterer) should be adjusted to

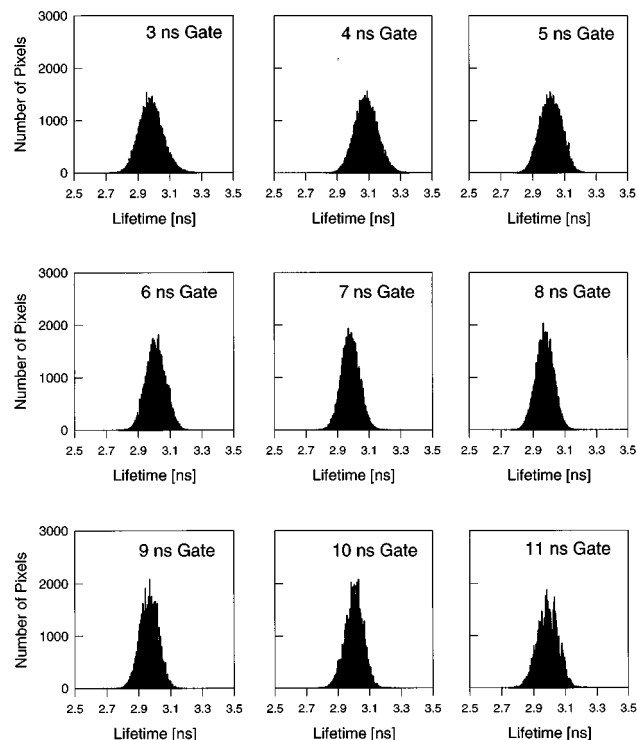


FIG. 7. Effect of the gate width on the quality of the lifetime image. The quality of the lifetime image (narrower histogram) is best for images of 7 and 8 ns gate width.

produce the same count rate so the instrument response will be the same for both measurements. The alignment of the laser beam with the microscope optics is critical. An incorrectly coupled laser beam will result in multiple reflections from lens surfaces which will reach the MCP-PMT at different times, introducing distortion in the system response. The usual full width half maximum of the system response is 70–100 ps. The collected specimen data were processed using the software package called GLOBAL.<sup>26</sup>

To validate our TRFLIM measurements, SPC and frequency-domain measurements (FD) of the same probes were also carried out and the results compared to those obtained using TRFLIM as well as to values, reported in the literature by other investigators (Table II). The lifetimes measured using TRFLIM and SPC are close to those reported in the literature and those obtained using FD; variation in the measurements is about 1%.

## VI. UTILITY OF LIFETIME IMAGING MEASUREMENTS

Using Rhodamine B as a probe, we obtained intensity and lifetime images as the focus ( $z$  position) in the microscope was varied (Fig. 8). While there was a clear change in intensity as the focus was changed, no change in the lifetime was observed. Thus, lifetime imaging is advantageous in that it is intensity invariant.

The TRFLIM and SPC instruments were also tested using the  $\text{Ca}^{2+}$  probe Calcium Crimson. The lifetimes of a series of solutions of varying  $\text{Ca}^{2+}$  concentrations containing equivalent amounts of Calcium Crimson were determined. The lifetime of Calcium Crimson is known to increase with

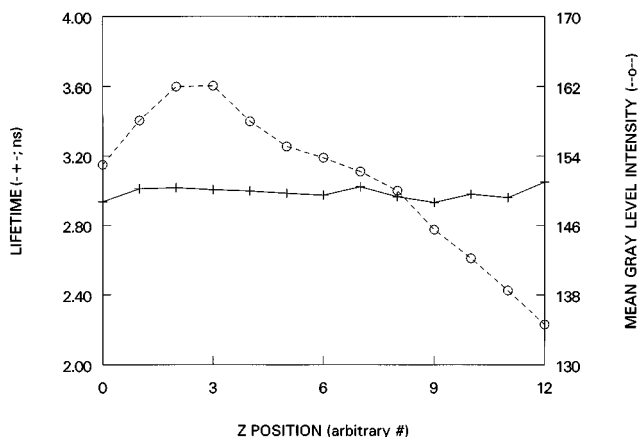


FIG. 8. Changes in intensity and lifetime as a function of focus. Changes in the focus (Z position) in the microscope leads to changes in intensity, but the lifetime remains constant. Lifetime measurements are thus independent of intensity.

increasing calcium concentration.<sup>17,27,28</sup> As previously discussed, lifetime measurements are relatively independent of signal intensity and concentration of the probe; measurement of  $\text{Ca}^{2+}$  using intensity measurements are not. Increases in probe concentration could be mistaken for an increase in  $\text{Ca}^{2+}$  when in fact the  $\text{Ca}^{2+}$  level remains the same. This is particularly worrisome when  $\text{Ca}^{2+}$  levels are being estimated using single wavelength  $\text{Ca}^{2+}$  probes such as Calcium Crimson. Figure 9 illustrates this problem. Figure 9(A) shows an intensity image of a cell labeled with the  $\text{Ca}^{2+}$ -sensitive probe Calcium Crimson; note that the nuclear region of the cell appears much brighter than the cytoplasm and would thus be assumed to have a higher level of  $\text{Ca}^{2+}$ . However, the lifetime image [Fig. 9(B)] demonstrates a fairly uniform lifetime of Calcium Crimson throughout the cell, indicative of a fairly uniform level of  $\text{Ca}^{2+}$ . This demonstrates one of the advantages of TRFLIM in that lifetime measurements, especially of single wavelength probes, are more accurate than intensity-based measurements. SPC lifetime measurements were also made in the nucleus and cytoplasm of single cells by illuminating either the nucleus or cytoplasm with a  $0.5 \mu\text{m}$  diameter laser beam spot. Results from these studies demonstrate that like TRFLIM, the lifetime of Calcium Crimson appears to be the same in the nucleus and the cytoplasm.<sup>27</sup>

## VII. APPLICATIONS

TRFLIM has potential applications in cell biology, clinical diagnostics, and other chemical analyses. Fluorescence lifetime probes are sensitive to numerous chemical and environmental parameters such as pH, oxygen, and  $\text{Ca}^{2+}$ , and thus TRFLIM can directly image the local environment (chemical and structural) immediately surrounding the probe. With respect to measuring  $\text{Ca}^{2+}$  in biological samples, TRFLIM allows the use of recently developed nonratiometric probes for  $\text{Ca}^{2+}$  such as Calcium Green, Calcium Crimson, and Calcium Orange.<sup>28,29</sup> These nonratiometric probes are extremely important for imaging the calcium concentration in cells using laser scanning confocal microscopy. The ratio-

metric calcium probes (Fura-2 and Indo-1) are excited by UV, which is not available in most laser scanning confocal microscopes. For example, the discovery of platelet-derived growth factor (PDGF) isoform-specific alterations in nuclear  $\text{Ca}^{2+}$  has recently been described based on the use of the  $\text{Ca}^{2+}$ -sensitive dye Fluo-3.<sup>30-32</sup> Fluo-3 cannot be employed as a ratiometric dye and thus quantitative calibrations of  $\text{Ca}^{2+}$  levels in cells is not possible. The use of TRFLIM allows measurement of regional variations in subcellular  $\text{Ca}^{2+}$  using single wavelength excitable  $\text{Ca}^{2+}$  probes, because  $\text{Ca}^{2+}$  concentration is derived from the lifetime and not the intensity of emission. TRFLIM also provides the opportunity to study the rotational mobility of a fluorescence lifetime probe using time-resolved emission anisotropy, providing the lifetime of the excited state is long enough.

TRFLIM can also be used to quantify the interaction, binding, or association of two types of molecules using fluorescence resonance energy transfer (FRET) spectroscopy.<sup>33-35</sup> FRET occurs through dipole-dipole interactions (nonradiative transfer of energy from one molecule to another) and is sensitive to the inverse sixth power of the distance between the two fluorophores; FRET occurs when the donor and acceptor molecules are within 10–100 Å of each other. The advantage of FRET measurements based on lifetimes as opposed to intensities is that the donor-acceptor distance is more accurately measured. By combining TRFLIM with FRET, it is possible to obtain quantitative temporal and spatial information about binding of proteins, lipids, enzymes, DNA, and RNA *in vivo*.

## VIII. DISCUSSION

We describe in this article the design and development of TRFLIM and its implementation in cell biological applications. TRFLIM is a noninvasive and powerful technique for the measurement of fluorescence lifetimes in two or three dimensions in biological and clinical specimens. The selection and assembly of the instrumentation are described as is its evaluation in measuring the fluorescent lifetime in comparison with more standard procedures for lifetime measurements. We detail the important steps one should consider in designing a TRFLIM instrument to measure lifetimes using pulsed excitation light sources. The short pulse width of the excitation laser pulses reduces photobleaching of the labeled probes in live cells as well as reduces error in measurements of subnanosecond lifetimes by the SPC method. The TRFLIM method requires only two windows (acquisition time  $< 2$  s) in a single decay curve to obtain the spatial distribution of average lifetimes. The simple algorithm presented here currently requires only 2 to 5 s to process and display high resolution ( $1000 \times 1000$ ) lifetime image on a color monitor. We estimate that by increasing the gating rate of the MCP-GII to 500 kHz and efficiently implementing the processing algorithm it would be possible to obtain and display lifetime images at video rate.

## ACKNOWLEDGMENTS

This work was supported by grants from the North Carolina Biotechnology Center, the American Cancer Society, the

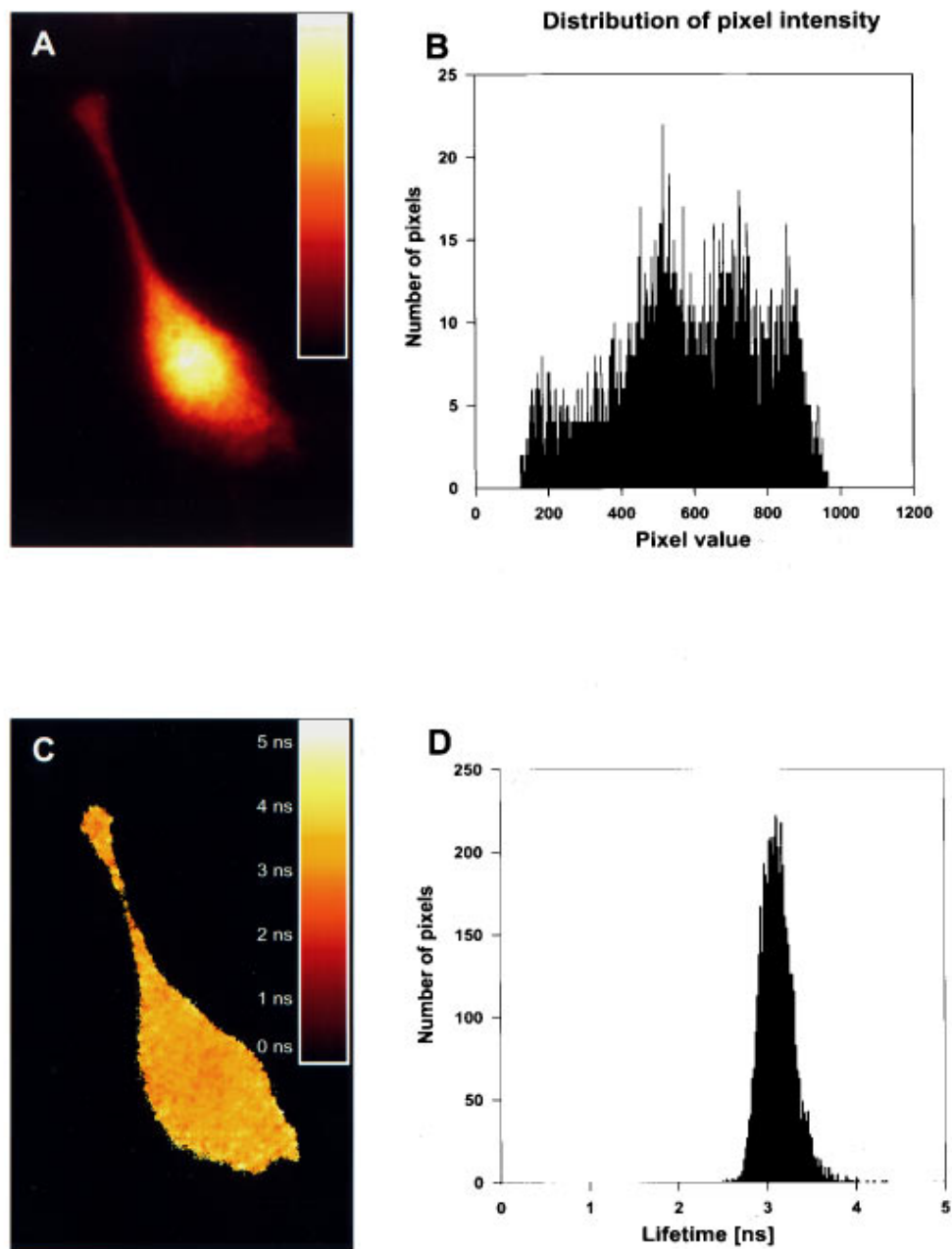


FIG. 9. Spatial distribution of intensity and lifetimes of Calcium Crimson in a single intact living BALB/c3T3 fibroblast. The cell was micro-injected with 30 mM Calcium Crimson, a  $\text{Ca}^{2+}$ -sensitive fluorescent indicator. (A) Time-resolved intensity image; (B) histogram of (A); (C) lifetime image; and (D) histogram of (C). The intensity measurement shows some spatial heterogeneity with respect to  $\text{Ca}^{2+}$  (i.e., the nucleus appears to have a higher level of  $\text{Ca}^{2+}$  based on its higher intensity). However, lifetime imaging demonstrates a relatively uniform level of  $\text{Ca}^{2+}$  throughout the whole cell.

National Science Foundation, the Gustavus and Louise Pfeiffer Research Foundation, the National Institutes of Health, and the Whitaker Foundation. We also wish to express our gratitude to Hamamatsu Photonics Systems, Bridgewater, NJ for their donation of the high-speed gated image intensifier used in this TRFLIM project. The authors also acknowledge Dr. Joseph Beechem, Vanderbilt University for useful discussions and Global analysis software for SPC.

<sup>1</sup>A. Periasamy and B. Herman, *J. Comput. Asst. Microsc.* **6**, 1 (1994).

<sup>2</sup>*Optical Microscopy: Emerging Methods and Applications*, edited by B. Herman and J. J. Lemasters (Academic, New York, 1993).

<sup>3</sup>R. Y. Tsien, *Annu. Rev. Neurosci.* **12**, 227 (1989).

<sup>4</sup>R. Y. Tsien, *Chem. Eng. News* July 18, 34 (1994).

<sup>5</sup>D. L. Taylor, M. Nederlof, F. Lanni, and A. S. Waggoner, *Am. Sci.* **80**, 322 (1992).

<sup>6</sup>A. Periasamy, M. Saidat-Pajouh, P. Wodnicki, X. F. Wang, and B. Herman, *Microsc. Anal.* March, 33 (1995).

<sup>7</sup>X. F. Wang, A. Periasamy, D. M. Coleman, and B. Herman, *Crit. Rev. Anal. Chem.* **23**, 369 (1992).

<sup>8</sup>*Principles of Fluorescence Spectroscopy*, edited by J. R. Lakowicz (Plenum, New York, 1986).

<sup>9</sup>L. B. McGown, *Anal. Chem.* **61**, 839A (1989).

<sup>10</sup>E. Gratton and M. Limkema, *Biophys. J.* **44**, 315 (1983).

<sup>11</sup>*Time-Correlated Single Photon Counting*, edited by D. V. O'Connor and D. Phillips (Academic, London, 1984).

<sup>12</sup>H. Kume, H. Nakamura, and M. Suzuki, in 19th International Congress on High-speed Photography and Photonics, *Proc. SPIE* **1358** (1991).

<sup>13</sup>R. M. Ballew and J. N. Demas, *Anal. Chem.* **61**, 30 (1989).

- <sup>14</sup>T. Ni and L. N. Melton, *Appl. Spectrosc.* **45**, 398 (1991).
- <sup>15</sup>X. F. Wang, T. Uchida, D. M. Coleman, and S. Minami, *Appl. Spectrosc.* **45**, 360 (1991).
- <sup>16</sup>T. Oida, Y. Sako, and A. Kusumi, *Biophys. J.* **64**, 676 (1993).
- <sup>17</sup>A. Periasamy, X. F. Wang, P. Wodnicki, G. W. Gordon, S. Kwon, P. A. Diliberto, and B. Herman, *J. Microsc. Soc. Am.* **1**, 13 (1995).
- <sup>18</sup>*Fluorescence Imaging Spectroscopy and Microscopy*, edited by X. F. Wang and B. Herman (Wiley, New York, 1996).
- <sup>19</sup>R. M. Clegg, B. Feddersen, E. Gratton, and T. M. Jovin, *Proc. SPIE* **1640**, 448 (1991).
- <sup>20</sup>M. C. Chang, S. H. Courtney, A. J. Cross, R. J. Gulotty, J. W. Petrich, and G. R. Fleming, *Anal. Instrum.* **14**, 433 (1985).
- <sup>21</sup>P. A. Diliberto, A. Periasamy, and B. Herman, in *Proceedings of the 49th Annual Meeting of the Electron Microscopic Society of America*, edited by G. W. Bailey and E. L. Hall (San Francisco Press, San Francisco, California, 1991), p. 228.
- <sup>22</sup>H. R. Haugen, B. W. Wallin, and F. E. Lytle, *Rev. Sci. Instrum.* **50**, 64 (1979).
- <sup>23</sup>U. P. Wild, A. R. Holzwarth, and H. P. Good, *Rev. Sci. Instrum.* **38**, 1621 (1977).
- <sup>24</sup>H. P. Good, A. J. Kallir, and U. P. Wild, *J. Phys. Chem.* **88**, 5435 (1984).
- <sup>25</sup>W. R. Laws, D. W. Potter, and J. C. Sutherland, *Rev. Sci. Instrum.* **55**, 1564 (1984).
- <sup>26</sup>J. M. Beechem, M. Ameloot, and L. Brand, *Anal. Instrum.* **14**, 379 (1985).
- <sup>27</sup>X. F. Wang, A. Periasamy, P. Woodnicki, G. W. Gordon, S. Kwon, P. A. Diliberto, and B. Herman, 34th Ann. Meet. Am. Soc. Cell Biol. **A48**, 124 (1994).
- <sup>28</sup>J. R. Lakowicz, H. Szmajnski, and M. L. Johnson, *J. Fluor.* **2**, 47 (1992).
- <sup>29</sup>J. R. Lakowicz and K. W. Berndt, *Rev. Sci. Instrum.* **62**, 3653 (1991).
- <sup>30</sup>P. A. Diliberto, S. Krishna, P. Wodnicki, and B. Herman, *Biophys. J.* **66**, A253 (1994).
- <sup>31</sup>P. A. Diliberto, X. F. Wang, and B. Herman, *Methods Cell Biol.* **40**, 243 (1994).
- <sup>32</sup>P. A. Diliberto and B. Herman, *Biophys. J.* **64**, A130 (1993).
- <sup>33</sup>I. Stryer, *Annu. Rev. Biochem.* **45**, 819 (1978).
- <sup>34</sup>B. Herman, *Methods Cell Biol.* **30**, 319 (1989).
- <sup>35</sup>T. M. Jovin and D. J. Arndt-Jovin, in *Cell Structure and Function by Microspectrofluorometry*, edited by E. Koken and J. G. Hirshberg (Academic, New York, 1989), p. 99.